

Physical Aspect of Exceptional Point in the Liouvillian Dynamics for a Quantum Lorentz Gas

Kazunari Hashimoto, Kazuki Kanki, Satoshi Tanaka
and Tomio Petrosky

Abstract Physical aspect of the exceptional point in the spectrum of the Liouville-von Neumann operator (Liouvillian) is discussed. The example we study in this paper is the weakly-coupled one-dimensional quantum perfect Lorentz gas. The effective Liouvillian for the system derived by applying the Brillouin-Wigner-Feshbach formalism takes non-Hermitian form due to resonance singularity, thus its spectra take complex values. We find that the complex spectra has two second order exceptional points in the wavenumber space. As a physical effect of the exceptional points, we show that the time evolution of the Wigner distribution function is described by the telegraph equation. The time evolution described by the telegraph equation shows a shifting motion in space. We also show that mechanism of the shifting motion completely changes at the exceptional points.

1 Introduction

In modern physics, the importance of non-Hermitian operator as a generator of motion has been recognized in many area of physics, both on an applied level and on a fundamental level. A typical example of the appearance of non-Hermitian operator is in a situation where we discuss irreversible processes. For example, in decaying processes in unstable systems, the effective Hamiltonian takes a non-Hermitian form

K. Hashimoto (✉)

Graduate School of Interdisciplinary Research, University of Yamanashi,
Kofu, Yamanashi 400-8511, Japan
e-mail: hashimotok@yamanashi.ac.jp

K. Kanki · S. Tanaka

Department of Physical Science, Osaka Prefecture University,
Sakai, Osaka 599-8531, Japan

T. Petrosky

Institute of Industrial Science, The University of Tokyo, Tokyo 153-8505, Japan

T. Petrosky

Center for Studies in Complex Quantum Systems, The University of Texas,
Austin 78712, USA

[1–3]. Non-Hermitian operator also plays a central role in PT (parity-time) symmetric systems [4–7].

In statistical mechanics, the Liouville-von Neumann operator (Liouvillian) generates time evolution of the distribution function, or of the density matrix [8]. As in the case of the effective Hamiltonian in open quantum systems, the effective Liouvillian takes a non-Hermitian form for thermodynamic systems where the intensive variables and the extensive variables exist in the thermodynamic limit [9].

Among many characteristic properties of the non-Hermitian operator, the appearance of the exceptional points in parameter space is especially interesting and it has been studied in many contexts in recent years [10–13]. The exceptional point is a singular point in the parameter space at which both eigenvalues and eigenvectors coalesce [10]. As a result, the non-Hermitian operator cannot be diagonalized at the point. Instead, the operator can be reduced to the Jordan block form. In the time evolution of the wave function in the Hamiltonian dynamics, the Jordan block leads to a linear time dependence besides the usual exponential time behavior as $t \exp[-\gamma t]$ [11]. Such time behavior at the exceptional point has been studied recently, for example, in [12] for an optical microcavity and in [13] for Rabi oscillation.

In our recent study, we have found that the exceptional point also appears in the spectrum of the Liouvillian for variety of physical systems both in quantum and classical mechanics. Such systems include the one-dimensional (1D) quantum perfect Lorentz gas [14], the two-dimensional classical perfect Lorentz gas [15] and the one-dimensional polaron system [16]. Although the physics of the exceptional point in Hamiltonian dynamics has been studied extensively, the study of the exceptional point in the Liouvillian dynamics is still in a poor level, as far as the authors knowledge.

The main purpose of this paper is to report our recent results on the physical effects of the exceptional points in the Liouvillian dynamics. The example we discuss in this paper is the weakly-coupled 1D quantum perfect Lorentz gas [14, 15]. The Lorentz gas is one of the simplest system that have the exceptional point in the spectrum of the Liouvillian.

In this paper, we shall show that the spectrum of the Liouvillian for the system has the second order exceptional points in the wavenumber space. We shall discuss physical effect of the exceptional points by analyzing time evolution of the Wigner distribution function. We shall show that the second order exceptional point leads to the telegraph equation in its spatial time evolution. There we shall also show that the time evolution of the distribution function in space shows a shifting motion, but its mechanism completely changes at the exceptional points; one is due to asymmetry of the momentum distribution function, while the other is due to wave propagation associated to the real part of the complex spectrum.

The structure of the paper is as follows: In Sect. 2, we introduce the model. In Sect. 3, we summarize essential formulae in the Liouville space description. In Sect. 4, we briefly summarize the complex spectral representation of the Liouvillian. In Sect. 5, we derive the effective Liouvillian for the system. In Sect. 6, we show a solution of the eigenvalue problem of the effective Liouvillian. In Sect. 7, we discuss the relation between the time evolution of the system and the exceptional points. In Sect. 8, we give a summary and a concluding remark.

2 System

We consider a weakly-coupled one-dimensional (1D) quantum Lorentz gas. The Lorentz gas consists of one light-mass particle (the test particle) with mass m and N heavy particles with mass M . We suppose that the system is enclosed in a large 1D box of volume L with the periodic boundary condition. The Hamiltonian of the system is given by

$$H = H_0 + gV = \frac{p^2}{2m} + \sum_{j=1}^N \frac{p_j^2}{2M} + g \sum_{j=1}^N \frac{1}{\Omega} \sum_n V_{q_n} e^{iq_n(x-x_j)}, \quad (1)$$

where g is a dimensionless coupling constant, $\Omega \equiv L/2\pi$ and $q_n \equiv n\Delta q$ with $\Delta q \equiv 1/\Omega$ and $n = 0, \pm 1, \pm 2, \dots$. The interaction is given by the Fourier expansion of $V(|x - x_j|)$ with $V_{q_n} = V_{|q_n|}$, which is assumed to be a short-range repulsive potential. We assume V_{q_n} is a continuous function at $q_n = 0$ in the continuous limit $\Delta q \rightarrow 0$, and satisfies the condition $O(|q_n|^{3/2}) < |V_{q_n}| < O(|q_n|^{1/2})$ for $q_n \rightarrow 0$, in order to avoid a singular transport process characteristic in 1D system. We also consider the weak-coupling situation ($g \ll 1$). In the following analysis, we restrict our attention to the limit $m/M \rightarrow 0$ in which the system is called the *perfect Lorentz gas* [17].

In this paper, we shall consider the thermodynamic limit,

$$L \rightarrow \infty, \quad N \rightarrow \infty, \quad c \equiv \frac{N}{L} = \text{finite}, \quad (2)$$

where c is the concentration of heavy particles. In this limit, we have $\Delta q \rightarrow 0$ and the wavenumber and the momentum become continuous variables. At an appropriate stage, we shall replace a summation with an integration and a Kronecker delta δ^{Kr} with a Dirac δ -function as

$$\frac{1}{\Omega} \sum_q \rightarrow \int dq, \quad \Omega_{\hbar} \delta^{Kr}(P - P') \rightarrow \delta(P - P'), \quad (3)$$

with $\Omega_{\hbar} \equiv \Omega/\hbar$ (Hereafter we use a conventional notation \sum_q for \sum_n and drop the index n in q_n).

In this paper we investigate the time evolution of the reduced density matrix for the test particle, which is defined as

$$f(t) \equiv \text{Tr}_{\text{hev}}[\rho(t)], \quad (4)$$

where $\rho(t)$ is the density matrix for the whole system and Tr_{hev} denotes a partial trace over all heavy particles. We assume that the initial condition of the system is given by

$$\rho(0) = f(0) \otimes \rho_{\text{hev}}^{eq}, \quad (5)$$

where ρ_{hev}^{eq} is the Maxwell distribution of the heavy particles with temperature T ,

$$\rho_{\text{hev}}^{eq} = \prod_{j=1}^N \frac{\exp(-p_j^2/2Mk_B T)}{\text{Tr}[\exp(-p_j^2/2Mk_B T)]}, \quad (6)$$

where k_B is the Boltzmann constant. In the thermodynamic limit the time evolution of the density matrix associated with the heavy particles is negligible since its deviation from ρ_{hev}^{eq} is proportional to $1/L$ in this limit, as can be easily shown.

3 The Liouville Space Description

The time evolution of the system is governed by the Liouville-von Neumann equation for the density matrix $\rho(t)$,

$$i \frac{\partial}{\partial t} \rho(t) = L_H \rho(t). \quad (7)$$

Here L_H is the Liouville-von Neumann operator (Liouvillean in short) which is defined by $L_H \rho \equiv [H, \rho]/\hbar$.

To discuss the space and momentum dependence of the distribution of the particles in parallel with classical mechanics, it is convenient to introduce the Wigner distribution function:

$$\rho^W(X, \{X_j\}, P, \{P_j\}, t) \equiv \frac{1}{L^{N+1}} \sum_{k, \{k_j\}} \rho_{k, \{k_j\}}(P, \{P_j\}, t) e^{i(kX + k_1 X_1 + \dots + k_N X_N)}, \quad (8)$$

which is a quantum analog of the phase space distribution function [9]. Here the notation $\{X_j\}$ represents a set of variables for the N heavy particles and

$$\begin{aligned} \rho_{k, \{k_j\}}(P, \{P_j\}, t) &\equiv \left\langle P + \frac{\hbar}{2} k, \left\{ P_j + \frac{\hbar}{2} k_j \right\} \middle| \rho(t) \middle| P - \frac{\hbar}{2} k, \left\{ P_j - \frac{\hbar}{2} k_j \right\} \right\rangle \\ &\equiv \langle\langle k, \{k_j\}; P, \{P_i\} | \rho(t) \rangle\rangle, \end{aligned} \quad (9)$$

where the single bra-ket vectors stand for vectors in the wave function space and the double bra-ket vectors stand for vectors in the Liouville space [9]. Here the ‘‘wavenumbers’’ and the ‘‘momenta’’ in the Wigner representation are defined as

$$k \equiv \frac{p - p'}{\hbar}, \quad P \equiv \frac{p + p'}{2}, \quad (10)$$

and the Wigner basis is defined by a dyad of two eigenstates of H_0 as

$$|k, \{k_j\}; P, \{P_j\}\rangle \equiv |p, \{p_j\}\rangle \langle p', \{p'_j\}|. \quad (11)$$

We represent a linear operator A in the wave function space as a ket-vector $|A\rangle\rangle$ in the Liouville space. The inner product of the bra- and ket-vectors is then defined by $\langle\langle B|A\rangle\rangle = \text{Tr}[B^\dagger A]$, where B^\dagger is the Hermitian conjugate of a linear operator B . As a result, it is easy to show that the Wigner basis vectors are normalized with respect to the box normalization condition

$$\begin{aligned} & \langle\langle k, \{k_j\}; P, \{P_j\} | k', \{k'_j\}; P', \{P'_j\} \rangle\rangle \\ &= \delta^{Kr}(k - k') \delta^{Kr}(P - P') \prod_{j=1}^N \delta^{Kr}(k_j - k'_j) \delta^{Kr}(P_j - P'_j). \end{aligned} \quad (12)$$

4 The Complex Spectral Representation of the Liouvillian

The eigenvalue problem of the Liouvillian is given by

$$L_H |F_\alpha^{(v)}\rangle\rangle = Z_\alpha^{(v)} |F_\alpha^{(v)}\rangle\rangle, \quad \langle\langle \tilde{F}_\alpha^{(v)} | L_H = \langle\langle \tilde{F}_\alpha^{(v)} | Z_\alpha^{(v)}, \quad (13)$$

where the indices α and ν specify an eigenstate (especially ν denotes the spatial correlation subspace (see [9])), and $|F_\alpha^{(v)}\rangle\rangle$ and $\langle\langle \tilde{F}_\alpha^{(v)} |$ are right- and left-eigenstates of the Liouvillian, respectively. We solve the eigenvalue problem of the Liouvillian by using the well-known Brillouin-Wigner-Feshbach formalism with projection operators $P^{(v)}$ and $Q^{(v)}$ satisfying the following relations,

$$P^{(v)} L_0 = L_0 P^{(v)}, \quad P^{(v)} P^{(\mu)} = \delta_{\nu,\mu}, \quad \sum_\nu P^{(\nu)} = \hat{I}_{N+1}, \quad P^{(v)} + Q^{(v)} = \hat{I}_{N+1}, \quad (14)$$

where \hat{I}_{N+1} is the unit operator for the $N + 1$ particle system. By applying these projection operators on the first equation in (13), we have

$$\Psi^{(v)}(Z_\alpha^{(v)}) P^{(v)} |F_\alpha^{(v)}\rangle\rangle = Z_\alpha^{(v)} P^{(v)} |F_\alpha^{(v)}\rangle\rangle, \quad (15)$$

where

$$\Psi^{(v)}(z) \equiv P^{(v)} L_H P^{(v)} + P^{(v)} L_H Q^{(v)} \frac{1}{z - Q^{(v)} L_H Q^{(v)}} Q^{(v)} L_H P^{(v)}, \quad (16)$$

is the *effective Liouvillian*. Its second term is the self-frequency part that corresponds to the self-energy part of an effective Hamiltonian in the case of the Hamiltonian operator in the wave function space. The effective Liouvillian is also called the *collision operator* which is a central object in the kinetic theory in non-equilibrium statistical mechanics [8, 9]. One can see from its eigenvalue equation (15) that the collision operator shares the eigenvalues with the Liouvillian. The eigenvalue

equation of the effective Liouvillian (15) is *non-linear*, i.e. the effective Liouvillian itself depends on the eigenvalue.

In terms of the right- and left-eigenstates of the effective Liouvillian $\Psi^{(v)}(z)$, the right- and the left-eigenvectors of the original Liouvillian L_H are given by

$$|F_\alpha^{(v)}\rangle = [P^{(v)} + \mathcal{C}^{(v)}(Z_\alpha^{(v)})]P^{(v)}|F_\alpha^{(v)}\rangle, \quad \langle\langle \tilde{F}_\alpha^{(v)}| = \langle\langle \tilde{F}_\alpha^{(v)}|P^{(v)}[P^{(v)} + \mathcal{D}^{(v)}(Z_\alpha^{(v)})], \quad (17)$$

where

$$\mathcal{C}^{(v)}(z) = \frac{1}{z - Q^{(v)}L_H Q^{(v)}}Q^{(v)}L_H P^{(v)}, \quad \mathcal{D}^{(v)}(z) = P^{(v)}L_H Q^{(v)}\frac{1}{z - Q^{(v)}L_H Q^{(v)}} \quad (18)$$

are the *creation-of-correlation operator* and the *destruction-of-correlation operator*, respectively, which are off-diagonal transitions between the $Q^{(v)}$ subspace and the $P^{(v)}$ subspace [9].

It is well-known for an unstable quantum system with a continuous spectrum that the effective Hamiltonian becomes a non-Hermitian operator due to the resonance singularity in the self-energy part [1]. Similarly, the effective Liouvillian becomes a non-Hermitian operator in the Liouville space in the thermodynamic limit. As a result, the effective Liouvillian has eigenstates with complex eigenvalues that are called *resonance states*. The imaginary part of the complex eigenvalue of the Liouvillian gives a transport coefficient of the system [18].

5 Effective Liouvillian for the System

We apply the general formalism presented above to the weakly-coupled 1D quantum perfect Lorentz gas. In the weak-coupling situation, the effective Liouvillian can be approximated up to the second order in g as

$$\Psi_2^{(k)}(z) = P^{(k)}L_0 P^{(k)} + g^2 P^{(k)}L_V Q^{(k)}\frac{1}{z - L_0}Q^{(k)}L_V P^{(k)}. \quad (19)$$

Here we define the projection operators as

$$P^{(k)} \equiv \frac{1}{\Omega_{\hbar}^{N+1}} \sum_{P, \{P_j\}} |k, \{0_j\}; P, \{P_j\}\rangle\langle\langle k, \{0_j\}; P, \{P_j\}|, \quad (20)$$

and $Q^{(k)} \equiv 1 - P^{(k)}$, where we have used the notation $\{0_j\}$ to indicate that all wavenumbers associated to the heavy particle are zero. For the projection operator $P^{(k)}$, we have

$$P^{(k)} L_0 P^{(k)} |k, \{0_j\}; P, \{P_j\}\rangle = \frac{kP}{m} |k, \{0_j\}; P, \{P_j\}\rangle, \tag{21}$$

and

$$P^{(k)} g L_V P^{(k)} = 0, \tag{22}$$

because of the condition $V_0 = 0$.

We focus our attention on the test particle, then we trace out the variables for the heavy particles. We also take the limit $m/M \rightarrow 0$ to obtain the perfect Lorentz gas. Thus we define the reduced effective Liouvillian for the 1D quantum perfect Lorentz gas as

$$\psi^{(k)}(z) \equiv \lim_{m/M \rightarrow 0} \text{Tr}_{\text{hev}} [\Psi_2^{(k)}(z) \rho_{\text{hev}}^{eq}]. \tag{23}$$

Expression of a matrix element of the reduced effective Liouvillian in the Wigner representation is given by

$$\begin{aligned} \langle\langle k; P | \psi^{(k)}(z) | k; P' \rangle\rangle &= \left[\frac{kP}{m} - \frac{2\pi g^2 c}{\hbar^2} \frac{1}{\Omega} \sum_{q \neq 0} |V_q|^2 \partial_P^{\hbar q/2} \frac{1}{z - (k - q)P/m} \partial_P^{\hbar q/2} \right] \\ &\times \delta_{\Omega \hbar}(P - P'), \end{aligned} \tag{24}$$

where we have dropped the variables for the heavy particles on the Wigner basis, and $\partial_P^{\hbar q/2} \equiv \hat{\eta}_P^{\hbar q/2} - \hat{\eta}_P^{-\hbar q/2}$ with $\hat{\eta}_P^{\hbar q/2} f(P) = f(P + \hbar q/2)$. Note that the expression (24) does not depend on the temperature of the heavy particles T . This is due to the limit of the perfect Lorentz gas $m/M \rightarrow 0$ where there is no energy exchange between the test particle and the heavy particles.

For the reduced effective Liouvillian, we write the eigenvalue problem as

$$\psi^{(k)}(z_\alpha^{(k)}) |u_\alpha^{(k)}\rangle = z_\alpha^{(k)} |u_\alpha^{(k)}\rangle, \quad \langle\langle \tilde{v}_\alpha^{(k)} | \psi^{(k)}(z_\alpha^{(k)}) = z_\alpha^{(k)} \langle\langle \tilde{v}_\alpha^{(k)} |, \tag{25}$$

We note that $z_\alpha^{(k)} = Z_\alpha^{(k)}$ for our Lorentz gas, because the heavy particles are in an eigenstate with zero eigenvalue, i.e. they remain in thermal equilibrium. The effective Liouvillian in (25) depends on its eigenvalue. In this sense, the eigenvalue equation is non-linear. Assuming bicompleteness in the subspace

$$\hat{p}^{(k)} \equiv \frac{1}{\Omega \hbar} \sum_P |k; P\rangle \langle\langle k; P|, \tag{26}$$

we can always construct sets of eigenstates $\{\langle\langle \tilde{u}_\alpha^{(k)} | \}$, which is biorthogonal to $\{|u_\alpha^{(k)}\rangle\}$, and $\{|v_\alpha^{(k)}\rangle\}$, which is orthogonal to $\{\langle\langle \tilde{v}_\alpha^{(k)} | \}$, with $\langle\langle \tilde{u}_\alpha^{(k)} | \neq \langle\langle \tilde{v}_\alpha^{(k)} |$ and $|v_\alpha^{(k)}\rangle \neq |u_\alpha^{(k)}\rangle$ [9].

6 Solution of the Eigenvalue Problem

6.1 The Boltzmann Approximation

In order to solve the eigenvalue problem (25), here we study a situation where the wavenumber k satisfies

$$|k| \ll d^{-1}, \quad (27)$$

where d is the interaction range between particles. In this situation in addition to the weak-coupling, we shall show that the eigenvalue dependence of the effective Liouvillian (24) is negligible and the non-linear eigenvalue problem (25) is linearized. There the effective Liouvillian is reduced to the phenomenological Boltzmann collision operator.

For a spatial inhomogeneity satisfying the condition (27), a typical value of q appearing in V_q is much larger than k in (24), i.e., $|k| \ll |q|$. Then we can neglect k in the denominator in the second term in (24). On the other hand, we may expect that the imaginary part of the eigenvalue z in (25) is proportional to g^2 for $g \ll 1$ because of the factor g^2 in front of the collision term in (24). If this is the case, we can evaluate z in (24) at $z = 0$. Then we have $\psi^{(k)}(z_\alpha^{(k)}) = \psi^{(k)}(+i0) + O(g^4)$. Here $+i0$ means that the collision operator $\psi^{(k)}(z)$ is evaluated on the real axis approaching from the upper half-plane of z to ensure the time evolution is oriented to the future $t > 0$ [9]. Combining these arguments, we can approximate $\psi^{(k)}(z_\alpha^{(k)})$ by the new operator given by

$$\begin{aligned} \langle\langle k; P | \psi_B^{(k)} | k; P' \rangle\rangle \equiv & \left[\frac{kP}{m} - \frac{2\pi g^2 c}{\hbar^2} \lim_{\epsilon \rightarrow +0} \int_{-\infty}^{\infty} dq |V_q|^2 \delta_P^{\hbar q/2} \frac{1}{+i\epsilon + qP/m} \delta_P^{\hbar q/2} \right] \\ & \times \delta(P - P'), \end{aligned} \quad (28)$$

where we have taken the thermodynamic limit (2). This is identical with the phenomenological Boltzmann collision operator for the 1D quantum perfect Lorentz gas [15, 19], for which the first term in the square bracket in (28) is called the flow term, and the second term is called Boltzmann's collision term.

By performing the q integration in (28), one can see that the Boltzmann collision operator has non-vanishing matrix elements only between the states $|k; P\rangle$ and $|k; -P\rangle$ [14]. Physically, this is because there are only forward and backward scattering in the 1D quantum system. Hence, in terms of these basis, the Boltzmann collision operator is represented by a 2×2 non-Hermitian matrix,

$$\psi_B^{(k)} = \begin{pmatrix} kP/m - ig^2\gamma_P/2 & ig^2\gamma_P/2 \\ ig^2\gamma_P/2 & -kP/m - ig^2\gamma_P/2 \end{pmatrix}, \quad (29)$$

with

$$g^2 \gamma_P \equiv g^2 \frac{8\pi^2 mc}{\hbar^2 |P|} |V_{\frac{2P}{\hbar}}|^2, \quad (30)$$

where $\gamma_P \rightarrow 0$ for $P \rightarrow 0$ due to the condition $V_0 = 0$.

In terms of the Boltzmann collision operator, the time evolution equation of the reduced density matrix is given by

$$i \frac{\partial}{\partial t} \hat{p}^{(k)} |f(t)\rangle\rangle = \psi_B^{(k)} \hat{p}^{(k)} |f(t)\rangle\rangle, \quad (31)$$

which is the Boltzmann equation for the system.

6.2 Eigenstates of the Boltzmann Collision Operator

Let us denote the right- and left-eigenstates of the collision operator (29) as $|\phi_\alpha^{(k)}\rangle\rangle$ and $\langle\langle \tilde{\phi}_\alpha^{(k)}|$, respectively, i.e.,

$$\psi_B^{(k)} |\phi_\alpha^{(k)}\rangle\rangle = z_\alpha^{(k)} |\phi_\alpha^{(k)}\rangle\rangle, \quad \langle\langle \tilde{\phi}_\alpha^{(k)}| \psi_B^{(k)} = z_\alpha^{(k)} \langle\langle \tilde{\phi}_\alpha^{(k)}|. \quad (32)$$

Here we present the solution of the eigenvalue problem and show that the solution has exceptional points in the wavenumber k space.

The characteristic equation for (29) is given by

$$\det[\psi_B^{(k)} - z \hat{I}_2] = \left(z + i \frac{g^2 \gamma_P}{2}\right)^2 - \left(\frac{kP}{m}\right)^2 + \left(\frac{g^2 \gamma_P}{2}\right)^2 = 0, \quad (33)$$

where \hat{I}_2 is the unit matrix of size 2. Hence, the eigenvalues are

$$z_{\pm;P}^{(k)} = -i \frac{g^2 \gamma_P}{2} \pm \frac{|P|}{m} (k^2 - k_P^2)^{1/2}, \quad (34)$$

where

$$k_P \equiv \frac{g^2 \gamma_P}{2|P|/m} = \frac{1}{l_P}, \quad (35)$$

is a wavenumber that is equal to the inverse of the mean-free-length of the test particle with momentum P denoted by l_P .

In Fig. 1, we show a k -dependence of the real part and the imaginary part of the eigenvalues for $P \neq 0$. In the figures, the dashed lines and the dot-dashed lines represent the eigenvalues $z_{+;P}^{(k)B}$ and $z_{-;P}^{(k)B}$, respectively. The solid lines represent that these two lines overlap.

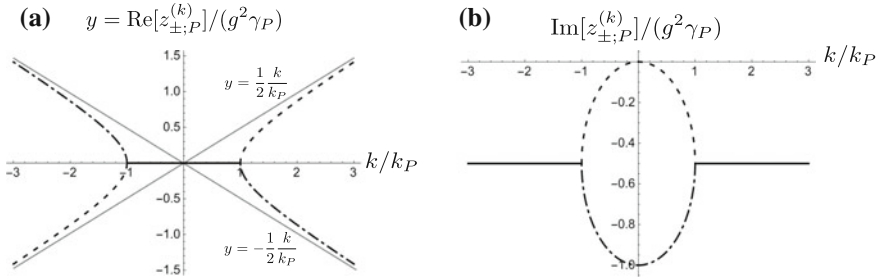


Fig. 1 Eigenvalues of the Boltzmann collision operator (34) are drawn as functions of k . **a** is the real part and **b** is imaginary part. In each figure, the *dashed lines* represent eigenvalue with $\alpha = +$ and the *dot-dashed lines* represent eigenvalue with $\alpha = -$. The *solid lines* represent that these two lines are overlapping. The *gray lines* in **a** represents eigenvalues of the Liouvillian for a free light-mass particle $y = \pm(1/2)(k/k_P)$

Corresponding right- and left-eigenvectors are

$$|\chi_{\pm;P}^{(k)}\rangle = \left[1 \pm \frac{(k^2 - k_P^2)_+^{1/2}}{k}\right]^{1/2} |k; |P|\rangle + i \frac{|k|}{k} \left[1 \mp \frac{(k^2 - k_P^2)^{1/2}}{k}\right]^{1/2} |k; -|P|\rangle, \tag{36a}$$

$$\langle\langle \tilde{\chi}_{\pm;P}^{(k)} | = \frac{|k|}{k} \left[1 \pm \frac{(k^2 - k_P^2)^{1/2}}{k}\right]^{1/2} \langle\langle k; |P| | + i \left[1 \mp \frac{(k^2 - k_P^2)^{1/2}}{k}\right]^{1/2} \langle\langle k; -|P| |. \tag{36b}$$

Here we have not yet normalized the eigenvectors by taking account of the fact that we have a diverging normalization constant at $k = \pm k_P$ (see (39)). The inner products of these right- and left-eigenstates are given by

$$\langle\langle \tilde{\chi}_{\pm;P}^{(k)} | \chi_{\pm;P'}^{(k)} \rangle = \pm \frac{2(k^2 - k_P^2)^{1/2}}{|k|} [\delta(P - P') + \delta(P + P')]. \tag{37}$$

Then, normalized eigenstates for $k \neq \pm k_P$ are given by

$$|\phi_{\pm;P}^{(k)}\rangle \equiv \sqrt{N_{\pm;P}^{(k)}} |\chi_{\pm;P}^{(k)}\rangle, \quad \langle\langle \tilde{\phi}_{\pm;P}^{(k)} | \equiv \sqrt{N_{\pm;P}^{(k)}} \langle\langle \tilde{\chi}_{\pm;P}^{(k)} |, \tag{38}$$

where the normalization constants are

$$N_{\pm;P}^{(k)} \equiv \pm \frac{|k|}{2(k^2 - k_P^2)^{1/2}}. \tag{39}$$

For $k \neq \pm k_P$, they satisfy the following bi-orthonormal and bi-completeness relations,

$$\langle\langle \tilde{\phi}_{\alpha;P}^{(k)} | \phi_{\alpha';P'}^{(k)} \rangle\rangle = \delta_{\alpha,\alpha'} [\delta(P - P') + \delta(P + P')], \quad \sum_{\alpha=\pm} \int_0^{\infty} dP |\phi_{\alpha;P}^{(k)}\rangle\langle\langle \tilde{\phi}_{\alpha;P}^{(k)} | = \hat{p}^{(k)}. \tag{40}$$

As a function of the wavenumber k , the eigenvalues (34) have the following two exceptional points on the real k axis,

$$k = \pm k_P. \tag{41}$$

At these points, both eigenvalues and eigenvectors coalesce. Since there is only one linearly independent eigenvector at these points, the Boltzmann collision operator (29) can not be diagonalized. Instead, the collision operator has the Jordan block structure at these points (see [3, 14]). This coalescence of eigenvectors does not take place at the usual degeneracy point of the eigenvalues of a Hermitian operator for which a degenerate eigenvalue is shared by two distinct eigenstates. In this sense, the exceptional point is often referred as the non-Hermitian degeneracy [20] In the previous paper [14], we have introduced a divergence free representation at exceptional points by continuously extending the Jordan block representation away from exceptional points.

7 A Physical Aspect of the Spectrum of the Liouvillian with the Exceptional Point

7.1 EP2 and the Telegraph Equation

In this subsection, we show that the second order exceptional point (EP2) in the spectrum of the Liouvillian leads to the telegraph equation, which has a hybrid nature of the diffusion equation and the wave equation. Let us first introduce the Wigner distribution function for the test particle,

$$f^W(X, P, t) \equiv \int_{-\infty}^{\infty} dk f_k(P, t) \equiv \int_{-\infty}^{\infty} dk \langle\langle k; P | f(t) \rangle\rangle. \tag{42}$$

We rewrite the characteristic equation of the collision operator (33) as

$$z^2 - ig^2\gamma_P z - |v|^2 k^2 = 0, \tag{43}$$

where $v \equiv P/m$. Its inverse Fourier transformation on the variables z and k leads to the telegraph equation

$$\frac{\partial^2}{\partial t^2} f^W(X, P, t) + g^2 \gamma_P \frac{\partial}{\partial t} f^W(X, P, t) = |v|^2 \frac{\partial^2}{\partial X^2} f^W(X, P, t). \quad (44)$$

In other words, the characteristic equation of the Boltzmann collision operator (43) is the same as the characteristic equation of the telegraph equation with regard to the X - and t -dependence as $\exp[i(kX - zt)]$. Hence our Boltzmann equation (31) is equivalent to the telegraph equation with regard to the dependence on the Wigner function on X and t . One can see that the telegraph equation reduces to the diffusion equation in long-time behavior in $t \gg (g^2 \gamma_P)^{-1}$ (see (50) as well as [14]).

The equivalence of the Boltzmann equation and the telegraph equation in their time development in X space is remarkable, since the telegraph equation represents a prototypical time behavior of the system with the EP2 in the spectrum of the Liouvillian with respect to the wavenumber. This is because, when the spectrum of the Liouvillian has the EP2 in the wavenumber space, the essential properties of the EP2 can be effectively described by a 2×2 matrix [21, 22], and the characteristic equation for the matrix always takes the quadratic form (43).

7.2 Time Evolution of the Wigner Distribution Function

As a demonstration of the time development of the system described by the telegraph equation, here we report a shifting motion of the Wigner distribution function localized in moderately small spatial scale less than the mean-free-length, but yet with a large enough width as compared with the microscopic scale given by the interaction range. We found shifting motion of the peak of the distribution function in space in addition to spreading as a result of a diffusion type process. However, the mechanism of the shifting motion completely changes at the exceptional points $k = \pm k_P$ as the following manner:

1. For $|k| \leq k_P$, the shifting motion comes from asymmetry in the momentum distribution before the momentum relaxation is complete.
2. For $|k| > k_P$, the shifting motion comes from the real part of the eigenvalue that leads to a wave propagation with the initial velocity P/m .

In order to see the above results, we consider the following situation as an initial condition,

$$f_k(P, 0) = \chi_{k_b}(k)h(P), \quad (45)$$

where $\chi_{k_b}(k)$ is a step function which is defined with a given value of k_b by $\chi_{k_b}(k) = 1$ for $|k| \leq k_b$ or $\chi_{k_b}(k) = 0$ for $|k| > k_b$, and $h(P)$ is a momentum distribution function that is normalized as

$$\int_{-\infty}^{\infty} dP h(P) = 1. \quad (46)$$

To extract the essence of the mechanism of the shifting motion, we here assume $h(P) = 0$ for $P < 0$, i.e., initial distribution is composed of particles with positive momentum.

The time evolution described by the telegraph equation (44) is also described by the Boltzmann equation (31). The formal solution of the Boltzmann equation is

$$\hat{p}^{(k)}|f(t)\rangle\rangle = e^{-i\psi_B^{(k)}t} \hat{p}^{(k)}|f(0)\rangle\rangle. \quad (47)$$

By multiplying $\langle\langle k; P|$ and using the completeness relation in (40), we have a special solution for the initial condition (45),

$$f_k(P, t) = \frac{1}{2} \left(e^{-iz_{+;P}^{(k)}t} + e^{-iz_{-;P}^{(k)}t} \right) f_k(P, 0) + \frac{kP}{m} \left(\frac{e^{-iz_{+;P}^{(k)}t} - e^{-iz_{-;P}^{(k)}t}}{z_{+;P}^{(k)} - z_{-;P}^{(k)}} \right) f_k(P, 0). \quad (48)$$

We use the units in which $l_P = 1/k_P = 1$ and $\tau_P = 1/(g^2\gamma_P) = 1$, when we present results of numerical calculations (see e.g. Fig. 2). With these units, the eigenvalues and the eigenvectors are independent of the value of P [23].

7.2.1 Time Evolution with the Spectrum in $|k| \leq K_P$

Let us first consider the situation where the initial distribution is composed of the Fourier components with k in the region $|k| \leq k_P$. Hence, we take $k_b \leq k_P$. In this case, the time evolution of the Wigner distribution function for $P > 0$ is expressed by

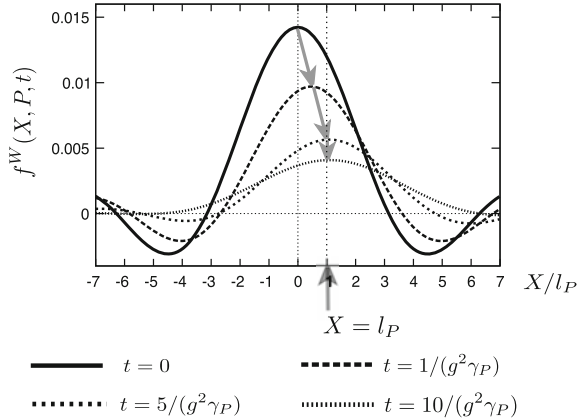
$$f^W(X, P, t) = \int_{-k_b}^{k_b} dk \frac{k_P}{2\sqrt{k_P^2 - k^2}} \left[e^{-iz_{+;P}^{(k)}t} \cos(kX - \varphi_{k,P}) + e^{-iz_{-;P}^{(k)}t} \cos(kX + \varphi_{k,P}) \right] \times f_k(P, 0), \quad (49)$$

with $\varphi_{k,P} \equiv \arctan[k/\sqrt{k_P^2 - k^2}]$.

In Fig. 2, we present the time evolution of (49) in X space with a specific value of momentum $P > 0$, which is implicitly given as a function of l_P and τ_P . In the figure, the solid line is the initial distribution, and the dashed lines are the distribution of later times. As shown in the figure, the peak of the distribution function shifts toward $X = l_P$ in the first stage of its time evolution. Afterwards, it stops the shifting motion with spreading its width with damping centering on the position of the peak, where the time evolution is described by the diffusion equation. This can be seen by the fact that (49) can be approximated after the above mentioned first stage as,

$$f^W(X, P, t) \simeq \int_{-\infty}^{\infty} dk \frac{1}{2} e^{-D_P k^2 t} \cos[k(X - l_P)] f_k(P, 0), \quad (50)$$

Fig. 2 Time evolution of the Wigner distribution function for $P > 0$. The *solid line* represents the initial distribution. The initial distribution is given by (45) with $k_b = k_p$. The initial distribution evolves to the distributions represented by the *dotted lines* as represented by the *arrows*



with

$$D_P \equiv \frac{g^2 \gamma_P}{4k_p^2} = \frac{(P/m)^2}{g^2 \gamma_P}, \tag{51}$$

which is a solution of the diffusion equation with a diffusion coefficient D_P [23].

We note that, for $t \rightarrow \infty$, the momentum distribution function is stationary as $f_0(P, t) = f_0(-P, t) = f_0(P, 0)/2$. This implies that the momentum relaxation has been completed, and this is the reason that the peak of the distribution no longer moves.

7.2.2 Time Evolution with the Spectrum in $|k| > k_p$

The eigenvalues (34) take complex values for $|k| > k_p$ and their real part approach to the eigenvalues of a free particle $\pm kP/m$ for $|k| \gg k_p$. Here we discuss how the structure of the spectrum affects to the time evolution of the system. For this purpose, we analyze time evolution with an initial condition (45) with $k_b > k_p$. For this initial condition, the time evolution of the Wigner distribution function for $P > 0$ can be divided into two parts; (i) f_d^W with pure imaginary eigenvalues and (ii) f_p^W with complex eigenvalues as

$$f^W(X, P, t) \equiv \int_{-\infty}^{\infty} dk f_k(P, t) e^{ikX} = f_d^W(X, P, t) + f_p^W(X, P, t), \tag{52}$$

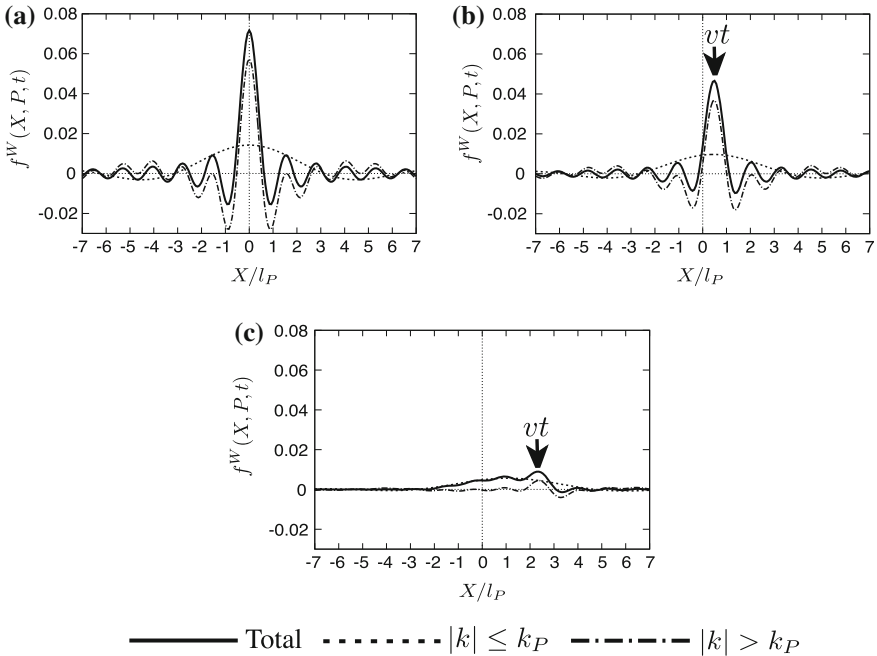


Fig. 3 Time evolution of the Wigner distribution function for $P > 0$. The initial distribution **a** is given by (45) with $k_b = 5.0k_p$. The distribution functions are shown for **a** $t = 0$, **b** $t = 1/(g^2\gamma_P)$ and **c** $t = 5/(g^2\gamma_P)$. In each figure, the solid line represents total value of the function f^W , the dashed line and the dot-dashed line represents f_d^W and f_p^W , respectively

with

$$f_d^W(X, P, t) \equiv \int_{-k_p}^{k_p} dk f_k(P, t) e^{ikX}, \quad f_p^W(X, P, t) \equiv \left(\int_{-k_b}^{-k_p} + \int_{k_p}^{k_b} \right) dk f_k(P, t) e^{ikX}. \tag{53}$$

In Fig. 3, we show the time evolution of f_d^W and f_p^W as well as the total distribution function f^W with a specific value of momentum $P > 0$. In each figure, the solid line represents the total distribution f^W , the dashed line represents f_d^W and the dot-dashed line represents f_p^W .

The time evolution of f_d^W has the same character as the time evolution of (49) discussed in the above subsection A, namely the distribution $f_d^W(X, P, t)$ firstly shifts toward $X = l_p$, within the time interval $0 \leq t \lesssim 1/(g^2\gamma_P)$. Afterwards, the distribution no longer shift and spreads its width by the diffusion process with its center fixed at l_p . On the other hand, the distribution $f_p^W(X, P, t)$ propagates as a wave packet with a velocity nearly equal to the initially given velocity P/m and decays in time. The wave propagation is due to the real part of the eigenvalues of the Liouvillian in the region $|k| > k_p$.

8 Summary and a Concluding Remark

In this paper, we have discussed physical significance of the exceptional point in the Liouvillian dynamics. The example we have studied is the weakly-coupled 1D quantum perfect Lorentz gas. We have solved the complex eigenvalue problem of the Liouvillian with a linear approximation where we approximate the effective Liouvillian by the Boltzmann collision operator. There we have shown that the spectrum has the second order exceptional points in the wavenumber space.

We have discussed the physical aspects of the exceptional points by studying the time evolution of the Wigner distribution function. There we have shown that when the Liouvillian of the system has the second order exceptional points in the wavenumber space, the time evolution obeys the telegraph equation. We have also shown that the time evolution described by the telegraph equation shows a shifting motion in space. There we have found two completely different mechanisms of the shifting motion; one is due to the asymmetry of the momentum distribution function, while the other is due to the wave propagation associated to the real part in the eigenvalue.

Among many properties of the exceptional point, the geometrical phase around it is especially interesting. Indeed, one can find many theoretical [2, 11, 20, 22, 24–32] and experimental papers [7, 13, 33–35] on this subject. However, all of these previous studies in this subject have been performed on the Hamiltonian level, and there is no study performed on the Liouvillian level. We hope to discuss this subject elsewhere.

References

1. N. Hatano, Fortschr. Phys. **61**, 238 (2013)
2. S. Garmon, I. Rotter, N. Hatano, D. Segal, Int. J. Theor. Phys. **51**, 3536 (2012)
3. G. Bhamathi, E.C.G. Sudarshan, Int. J. Mod. Phys. B **10**, 1531 (1996)
4. S. Klaiman, U. Gunther, N. Moiseyev, Phys. Rev. Lett. **101**, 080402 (2008)
5. G.D. Valle, S. Longhi, Phys. Rev. A **87**, 022119 (2013)
6. O. Vázquez-Candanedo et al., Phys. Rev. A **89**, 013832 (2014)
7. B. Peng et al., Nat. Phys. **10**, 394 (2014)
8. I. Prigogine, Non-equilibrium statistical mechanics (Wiley, 1962)
9. T. Petrosky, I. Prigogine, Adv. Chem. Phys. **99**, 1 (1997)
10. T. Kato, *Perturbation Theory of Linear Operators* (Springer, Berlin, 1966)
11. W.D. Heiss, Eur. Phys. J. D **60**, 257 (2010)
12. J. Wiersig, S.W. Kim, M. Hentschel, Phys. Rev. A **78**, 53809 (2008)
13. B. Dietz et al., Phys. Rev. E **75**, 027201 (2007)
14. K. Hashimoto et al., Prog. Theor. Exp. Phys. **2015**, 023A02 (2015)
15. Z.L. Zhang, Irreversibility and extended formulation of classical and quantum nonintegrable dynamics, Ph.D. Thesis, The University of Texas at Austin, 1995
16. Y. Sato, K. Kanki, S. Tanaka, T. Petrosky, unpublished
17. R. Balescu, *Statistical Mechanics of Charged Particles*, (Wiley, 1963)
18. T. Petrosky, Prog. Theor. Phys. **123**, 395 (2010)
19. R. Esposito, M. Pulvirenti, A. Teta, Commun. Math. Phys. **204**, 619 (1999)

20. M.V. Berry, Czech. J. Phys. **57**, 1039 (2004)
21. W.D. Heiss, W.H. Steeb, J. Math. Phys. **32**, 3003 (1991)
22. W.D. Heiss, Eur. Phys. J. D **7**, 1 (1999)
23. K. Hashimoto, K. Kanki, S. Tanaka, T. Petrosky, [arXiv:1507.02038](https://arxiv.org/abs/1507.02038)
24. W.D. Heiss, A.L. Sannino, J. Phys. A: Math. Gen. **23**, 1167 (1990)
25. W.D. Heiss, J. Phys. A: Math. Gen. **37**, 2455 (2004)
26. H. Cartarius, J. Main, G. Wunner, Phys. Rev. Lett. **99**, 173003 (2007)
27. J. Rubinstein, P. Sternberg, Q. Ma, Phys. Rev. Lett. **99**, 167003 (2007)
28. W.D. Heiss, J. Phys. A: Math. Theor. **41**, 244010 (2008)
29. R. Lefebvre, O. Atabek, M. Sindelka, N. Moiseyev, Phys. Rev. Lett. **103**, 123003 (2009)
30. H. Cartarius, N. Moiseyev, Phys. Rev. A **84**, 013419 (2011)
31. G. Demange, E. Graefe, J. Phys. A: Math. Theor. **45**, 025303 (2012)
32. I. Gilary, A.A. Mailybaev, N. Moiseyev, Phys. Rev. A **88**, 010102 (2013)
33. C. Dembowski et al., Phys. Rev. Lett. **86**, 787 (2001)
34. C. Dembowski et al., Phys. Rev. Lett. **90**, 034101 (2003)
35. J. Schindler, A. Li, M.C. Zheng, F.M. Ellis, T. Kottos, Phys. Rev. A **84**, 040101 (2011)